CONTINUOUS LASER HARDENING WITH INDUCTION PRE-HEATING

Doležel I.[1], Kotlan V.[2], Hamar R.[2], Pánek D.[2]
[1] Czech Technical University, Prague, Czech Republic, dolezel@fel.cvut.cz
[2] University of West Bohemia, Pilsen, Czech Republic, {vkotlan, hamar, panek50}@kte.zcu.cz

Annotation: **A novel way of continuous surface hardening of steel bodies by a laser beam is modeled. This heat treatment is supplemented with pre-heating of the hardened parts by a classic inductor in order to reduce the temperature gradients and subsequent mechanical stresses in the processed material. The mathematical model of the process is solved numerically in 3D and the solution respects all important nonlinearities (a saturation curve of the hardened steel and temperature dependences of its physical properties). The methodology is illustrated with a typical example, whose results are presented and discussed.**

Keywords: **laser hardening, induction heating, hard-coupled problem, numerical analysis, magnetic field, temperature field.**

INTRODUCTION

Laser surface hardening of steel bodies has been developing for more than ten years and became very popular in many industrial applications. This way of heat treatment exhibits numerous advantages, such as a good possibility of controlling the velocity and direction of the laser beam movement, power of the beam, and fast cooling by the transfer of heat from the surface to the interior of the body [1], [2]. The unit power delivered by the laser beam is even by six orders higher than power produced by classic induction heating by inductors. On the other hand, extremely fast heating of the surface (and also its consequent cooling) brings about undesirably high internal mechanical strains and stresses in the surface layers of the processed material.

In order to suppress the above-mentioned phenomena, an additional technology has been introduced, consisting in the induction pre-heating of the most exposed parts of the heated body. One of the arrangements of the process based on combined heating is depicted in Pic. 1. A system inductor-laser moves at a slow velocity $\boldsymbol{v}$ along the surface of the processed body. First, the body is pre-heated by the inductor of a suitable shape to a temperature ranging usually between 150–350 °C, then it is heated by the laser beam above the austenitizing temperature Ac_3, at which the material obtains a uniform austenite structure. The required hardness of the surface layers is then given by the time of cooling below the martensite temperature M_s (which usually takes several seconds). The resultant hardness generally grows with the velocity of cooling.

FORMULATION OF TECHNICAL PROBLEM

The task is to map the process of hardening a thin strip on a planar surface of a large workpiece using the combination of the induction pre-heating, laser heating and induction post-heating. The pre-heating and post-heating are performed by inductors of suitable shapes that move at the prescribed distance above the surface. The laser head connected firmly with the system of inductor is fixed between the inductors and moves with them.

The paper presents the mathematical model of the process and maps the time evolution of temperature along the beam trace.

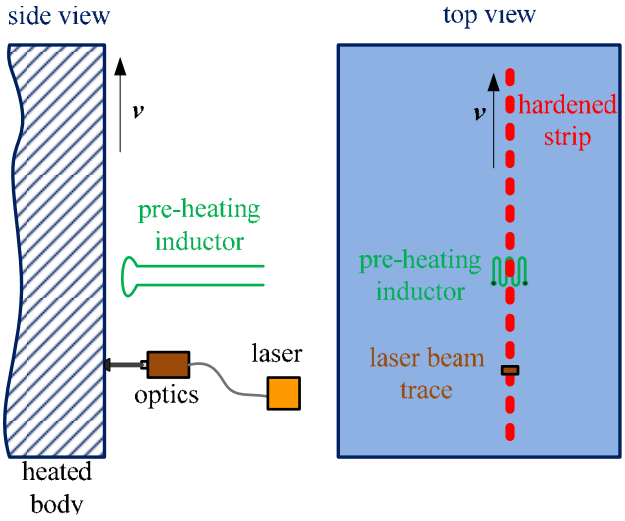

Pic. 1. Laser hardening with induction pre-heating

MATHEMATICAL MODEL OF THE PROCESS

From the physical viewpoint, the process represents a coupled nonlinear problem characterized by a hard interaction of the magnetic and temperature fields mutually influencing each other.

Its continuous mathematical model consists of two sub-models. The first one models the process of the induction pre-heating, the other one models the laser heating. The first sub-model consists of two second-order partial differential equations describing the distribution of the magnetic and temperature fields.

The distribution of magnetic field may be described in terms of several quantities. For example, it may be modeled by the magnetic vector potential $\boldsymbol{A}$ using the equation [3]

$$\operatorname{curl}\left(\frac{1}{\mu}\operatorname{curl}\boldsymbol{A}\right)+\gamma\left(\frac{\partial\boldsymbol{A}}{\partial t}-\boldsymbol{v}\times\operatorname{curl}\boldsymbol{A}\right)=\boldsymbol{J}_{ext} \qquad (1)$$

where μ is the magnetic permeability, γ denotes the electric conductivity, $\boldsymbol{v}$ is the vector of velocity of the system, and $\boldsymbol{J}_{ext}$ stands for the vector of the external current density in the field coils (which is, for the sake of simplicity, considered harmonic).

But solution to (1) is, in this particular case, practically unfeasible. The main reason is the deep disproportion between the frequency f (usually tens of kHz) of the field current I_{ext} carried by the inductors and the time of pre-heating or post-heating the surface layers of the body (in the order of seconds). The computation of one variant in 3D would therefore take unacceptable time in the order of weeks. That is why the model was somewhat simplified using the assumption that the magnetic field is harmonic, which allows solving the problem in the frequency domain. Then the magnetic field distribution can be described by the Helmholtz equation for the phasor $\underline{\boldsymbol{A}}$ of the magnetic vector potential $\boldsymbol{A}$ [4]

$$\operatorname{curl}\left(\operatorname{curl}\underline{\boldsymbol{A}}\right)+\gamma\mu\left(\mathrm{j}\cdot\omega\underline{\boldsymbol{A}}-\boldsymbol{v}\times\operatorname{curl}\underline{\boldsymbol{A}}\right)=\mu\underline{\boldsymbol{J}}_{ext}. \qquad (2)$$

Here, the symbol ω represents the angular frequency ($\omega=2\pi f$). But the magnetic permeability of ferromagnetic parts is not supposed to be a constant everywhere; its value is always assigned to the local value of magnetic flux density $|\boldsymbol{B}|$ in every element of the discretization mesh. Its value is, in such a case, based on a relevant iterative procedure computed in all good electromagnetic codes.

Here, the above-mentioned formulation is used because the task is solved using COMSOL Multiphysics. It is, however, necessary to point out that the description of 3D magnetic fields completely by the magnetic vector potential $\boldsymbol{A}$ is not very suitable; the reason consists in the necessity of a very high memory and computational time. This is due to the fact that at every point of the discretization mesh we must search three components of this quantity. Most of the specialized professional codes (FLUX, OPERA and others) use methods working with an appropriate version of either $\boldsymbol{A}-\varphi$ formulation or $\boldsymbol{T}-\Omega$ formulation [5], [6]. This means that in electrically conductive regions the magnetic field is described by either the magnetic vector potential $\boldsymbol{A}$ or electric vector potential $\boldsymbol{T}$, while linear electrically nonconductive regions are described by either the scalar electric potential φ or scalar magnetic potential Ω. The connection between both vector and scalar quantities is given through the conditions for the field vectors along the corresponding interfaces. In this way, a lot of the degrees of freedom (DOFs) can be saved and application of suitable algorithms may even lead to a substantial acceleration of iteration processes in nonlinear domains.

Any indicated formulation, however, requires correct boundary conditions for the processed quantities. In the case of the magnetic vector potential $\boldsymbol{A}$, the artificial boundary (placed at a sufficient distance from the system) is of the Dirichlet type ($\boldsymbol{A}=\boldsymbol{0}$). When symmetries are present, the condition along the faces is of the Neumann type. In the solved problem we can (without any significant error) neglect the velocity term in (2), because for small velocities in the order of mm/s its value is quite negligible with respect to the transformation term.

The temperature field in the heated body obeys the equation [7]

$$\operatorname{div}\left(\text{л}\cdot\operatorname{grad}T\right)=\text{c}c_p\cdot\left(\frac{\partial T}{\partial t}+\boldsymbol{v}\cdot\operatorname{grad}T\right)-w, \qquad (3)$$

where л is the thermal conductivity, c denotes the mass density, and c_p stands for the specific heat (all of these parameters are generally temperature-dependent functions). Finally, the symbol w denotes the time average internal volumetric sources of heat that generally consist of the volumetric Joule losses w_J (due to eddy currents) and magnetization losses w_m. In other words,

$$w=w_J+w_m, \quad w_J=\frac{\left|\underline{\boldsymbol{J}}_{eddy}\right|^2}{\text{г}}, \quad \underline{\boldsymbol{J}}_{eddy}=\mathrm{j}\cdot\text{ш}\text{г}\underline{\boldsymbol{A}}, \qquad (4)$$

where the losses w_m (if they are considered) are determined either from the known measured loss dependence $w_m=w_m\left(\left|\underline{\boldsymbol{B}}\right|\right)$ for the material used, or using a suitable (for example Steinmetz) formula. The boundary conditions respect convection and radiation.

Unlike the magnetic field, the velocity term in (3) cannot be neglected, even for very small velocities.

The other sub-model describes the distribution of the temperature field produced by the laser beam. Now the heat transfer equation has the form

$$\operatorname{div}\left(\text{л}\cdot\operatorname{grad}T\right)=\text{c}c_p\cdot\left(\frac{\partial T}{\partial t}+\boldsymbol{v}\cdot\operatorname{grad}T\right), \qquad (5)$$

because the internal sources of heat vanish. The source of heat is now the heat flux $\boldsymbol{q}_{in}$ entering the surface of the heated body at the place of impact of the laser beam. This is given by the boundary condition

$$-\text{л}\frac{\partial T}{\partial n}=\left|\boldsymbol{q}_{in}\right|, \qquad (6)$$

where n denotes the outward normal. The same may be used for determining the local heat flux $\boldsymbol{q}_{out}$ due to convection and radiation expressed by another boundary condition

$$-\text{л}\frac{\partial T}{\partial n}=\left|\boldsymbol{q}_{\text{out}}\right|=\text{б}_{gen}\left(T-T_{ext}\right). \qquad (7)$$

Here, the symbol б_{gen} stands for the generalized coefficient of the convective heat transfer (which also includes the influence of radiation) and T_{ext} stands for the temperature of ambient air. The prescription of the boundary conditions requires knowledge of the surface temperature of the body after pre-heating, which is somewhat reduced by cooling caused by the local time delay between the pre-heating and laser heating.

NUMERICAL SOLUTION

The numerical solution of the mathematical model consisting of (2), (3), (5) and corresponding boundary conditions was solved by professional code COMSOL Multiphysics 4.3 [8]. The solution in the hard-coupled formulation was carried out by the second-order finite

element method. During the computations, numerous mathematical indicators were carefully monitored, such as the convergence of the results (three valid figures) in the dependence on the density of the discretization mesh and position of the artificial boundary, stability of the time integration, etc. The computation of one variant of a selected example took a top-quality PC four or five hours.

ILLUSTRATIVE EXAMPLES

The task requires an efficient strategy, because computations, processing and comparison of the results are highly demanding business. Unfortunately, particular variants may differ in the heated material (and its characteristics), mutual geometrical position of the laser and both inductors, velocity v of the system current in the inductors, shielding elements and many other factors.

That is why we (as for heated materials) confined to two typical carbon steels (of makes ČSN 12 040 produced in the Czech Republic and AISI 4130 produced in Germany). The heating itself was conducted on a large massive plate made of one of these materials.

EXAMPLE 1

First, we decided to obtain a good idea about the time evolution of temperature during the pure laser heating of a small surface of steel ČSN 12 040. The laser did not move, see Pic. 2. The results were compared with experimental data measured in the cooperating company MATEX PM (Pilsen).

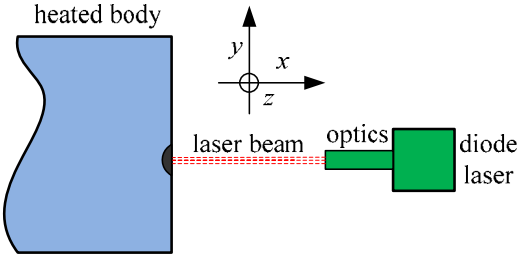

Pic. 2. Heating by static laser beam (without inductors)

The body in the form of a plate has dimensions 43 mm in the x direction, 21 mm in the y direction, and 102 mm in the z direction. The maximum output of the diode laser was $P_{max} = 3.5\,\text{kW}$ with the efficiency of 35%. For the comparison, we used a steady-state power of 1.925 kW at the same efficiency, which is a typical value commonly applied for hardening. The width of the laser beam was 5 mm. The time of heating was 3 s and then the laser was switched off.

The heated plate was made of carbon steel CSN 12 040 (Czech make), whose parameters are temperature-dependent functions presented in Pics. 3–5. Its austenitizing temperature is $\text{Ac}_3 = 755\,°\text{C}$. Finally, the value of $\sigma_{gen} = 10$ $\text{Wm}^{-2}\text{K}^{-1}$. In the process of heating, the temperature of the heated spot should exceed 1200 °C, but it should not be higher than 1400 °C.

The mathematical model is represented just by (5) (we do not work with the magnetic field). The computations were carried out in the environment of code COMSOL 4.3 supplemented with a number of special procedures and scripts designed in-house. The principal results are depicted in Pic. 6. The time evolution of the heated spot well corresponds with the measured data. The difference at the beginning of the process is caused by the fact that the pyrometer was able to correctly measure only from temperatures about 800 °C.

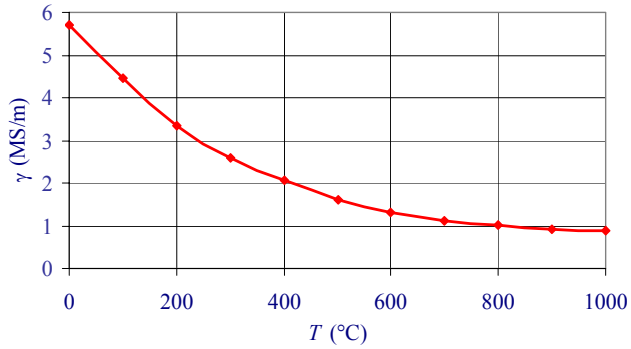

Pic. 3. Electric conductivity versus temperature (carbon steel ČSN 12 040)

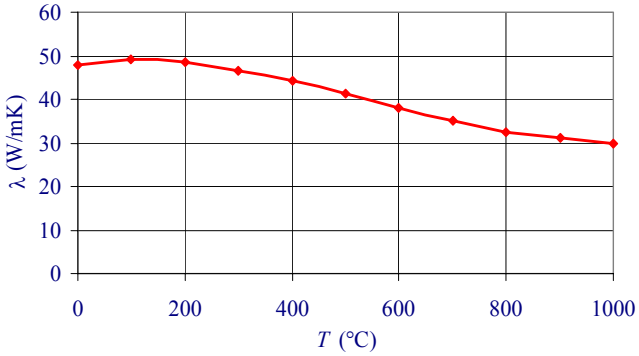

Pic. 4. Thermal conductivity versus temperature (carbon steel ČSN 12 040)

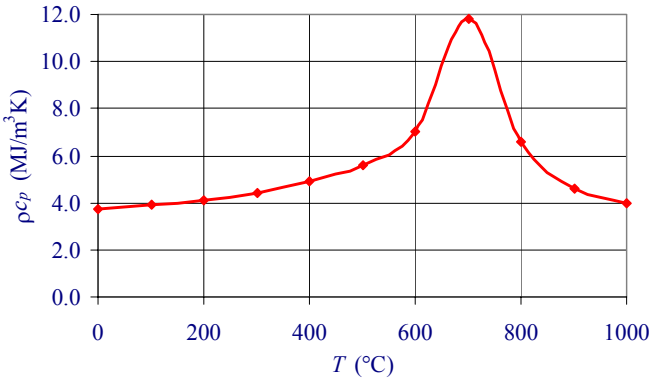

Pic. 5. Heat capacity versus temperature (carbon steel ČSN 12 040)

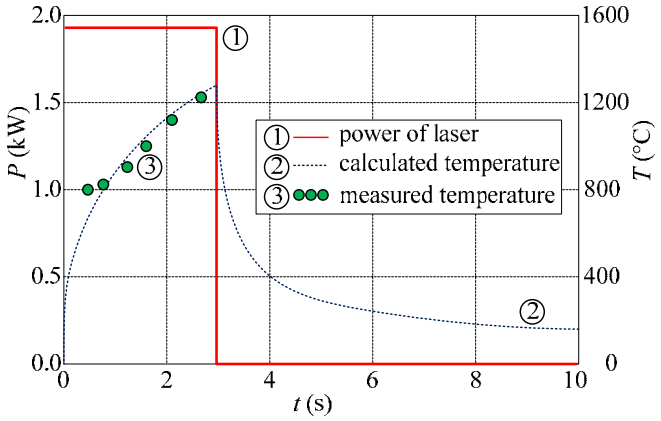

Pic. 6. Time evolution of laser power and temperatures in heated place

It can be seen that the growth of the temperature at the beginning of the process of heating is very high (it exceeds 1000 °C/s), which could produce in the surface layers undesirable mechanical stresses of a thermoelastic origin. That is why appropriate measures must be taken for suppressing that high temperature variation.

EXAMPLE 2

The goal of the other example is to map the time evolution of temperature along a given strip during the combined process consisting of the inductor pre-heating and laser heating.

The basic arrangement of the steel plate and heating system is depicted in Pic. 7.

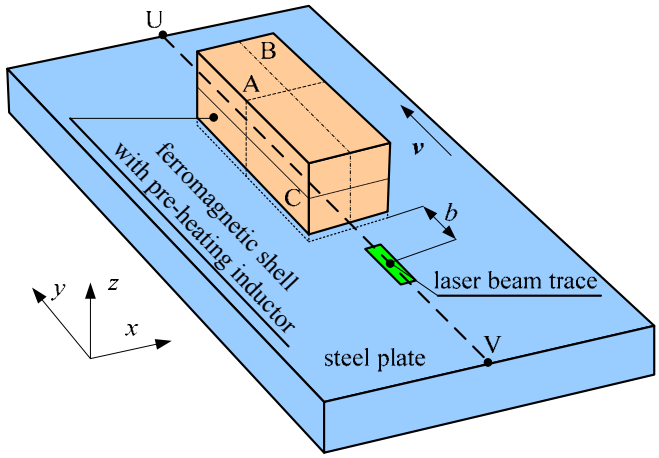

Pic. 7. Arrangement of investigated system

The plate is made of carbon steel AISI 4130. Its most important temperature-dependent characteristics are shown in Pics. 8–11.

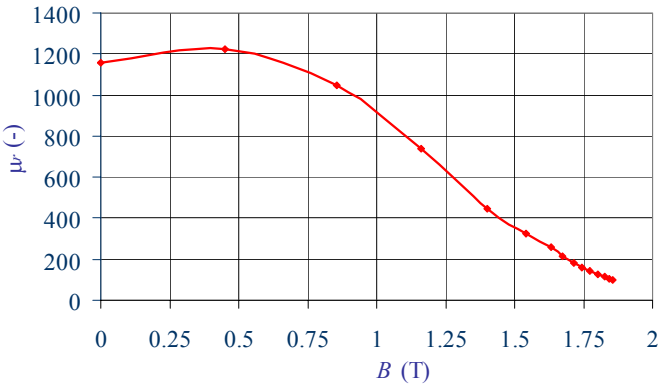

Pic. 8. Saturation curve of steel AISI 4130

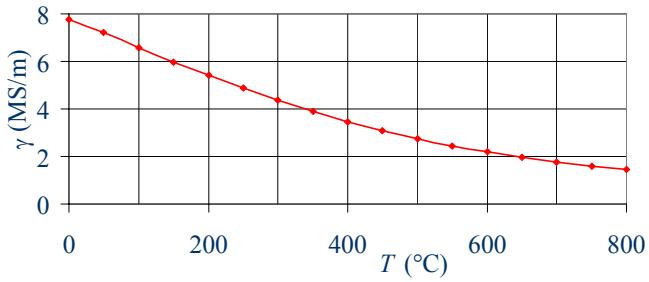

Pic. 9. Electric conductivity versus temperature (carbon steel AISI 4130)

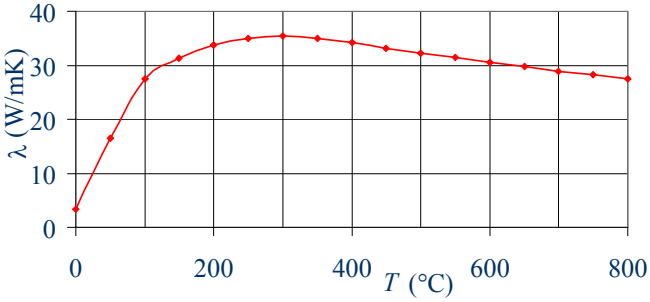

Pic. 10. Thermal conductivity versus temperature (carbon steel AISI 4130)

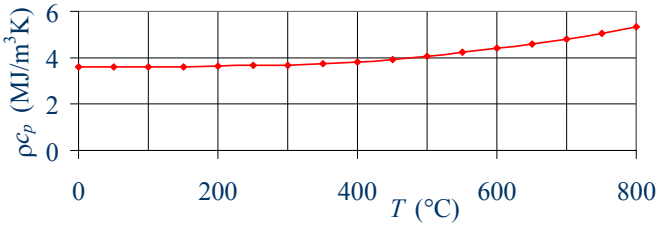

Pic. 11. Heat capacity versus temperature (carbon steel AISI 4130)

The field coil has 12 turns of a copper rope of diameter $d = 6$ mm consisting of many thin mutually insulated conductors in order to avoid an excessive skin effect. The coil is placed in a flux concentrator made of low-electrically conductive ferrite (the purpose is to suppress in its structure the Joule losses generated by the induced currents). Its dimensions and full arrangement follow from Pic. 12 showing this element in three cuts A, B and C marked in Pic. 7. Shown are also the dimensions of the laser beam trace S .

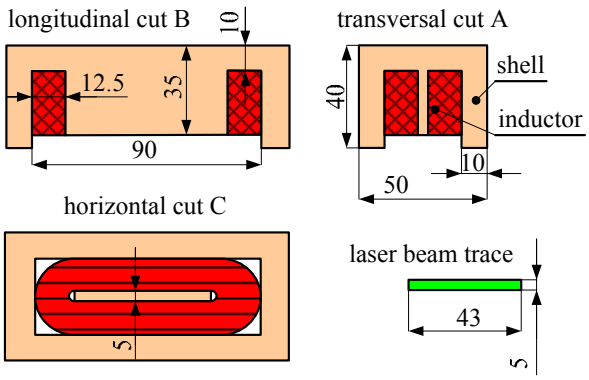

Pic. 12. Principal dimensions of field coil and concentrator

The nominal power of the laser beam transferred to the plate is $P = 1.4$ kW (corresponding to the real laser device at the company MATEX PM Pilsen) with the power density

$$p = \frac{P}{S} = \frac{1400}{5 \times 43 \times 10^{-6}} = 6.512 \text{ MW/m}^2.$$

where S is the area of the laser beam trace.

During the process of pre-heating, the surface of steel in the place of the laser beam trace should reach temperatures about 300 °C, which is the condition for reducing the subsequent mechanical stresses in the material. There are several factors influencing this quantity, as well as the thickness of the hardened layer. In addition to the parameters (amplitude and frequency) of the field current, important are also the velocity v of motion of the system and distance between the inductor and laser beam trace. This velocity, moreover, must be selected with respect to the requirement that the maximum surface temperature in the laser beam trace must not exceed 1400 °C.

After numerous preliminary computations (considering various technological constraints) we selected the following parameters: $I = 150$ A, $f = 10$ kHz, $v = 1$ mm/s (the system moves in the direction of the y axis) and the distance between the rear wall of the inductor and center of the laser beam trace (see Fig. 7) $b = 25$ mm.

As the inductor heats the material only to temperatures not exceeding about 350 °C, it is not necessary to consider the dependence of its magnetic permeability on temperature (its Curie temperature $T_C = 670$ °C). The initial temperature is $T_0 = 21$ °C, the convective coefficient $\alpha = 15$ W/m^{2}K, and the emissivity $C = 0.7$.

Pics. 13–15 show the models of the coil, concentrator and the whole system in the environment of code COMSOL Multiphysics 4.3. As the coil is manufactured of a copper rope consisting of thin wires, the distribution of the current density along its cross section may be considered uniform. That is why its model can be geometrically simplified to the form depicted in Pic. 13. Here, the current density was determined from the condition that the current content corresponds to 12 turns of the real coil. Pic. 14 shows the model of the ferrite concentrator and Pic. 15 shows the complete system.

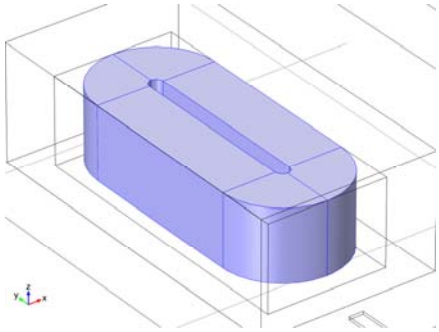

Pic. 13. Model of field coil in COMSOL Multiphysics

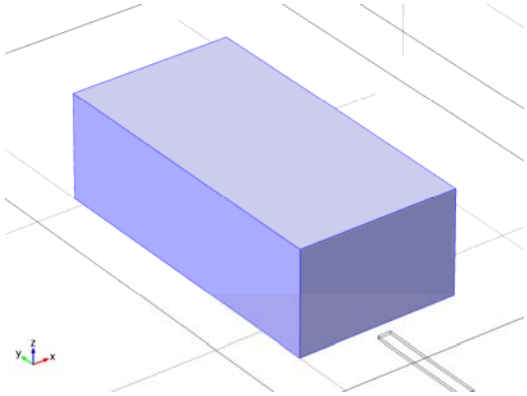

Pic. 14. Model of concentrator in COMSOL Multiphysics (laser beam trace can partially be seen right below)

The discretization mesh of the arrangement consisted of over 80000 second-order elements, the number of DOFs was about 230000 and the time of computation was over 4 hours. The requirements on the accuracy of results were satisfied.

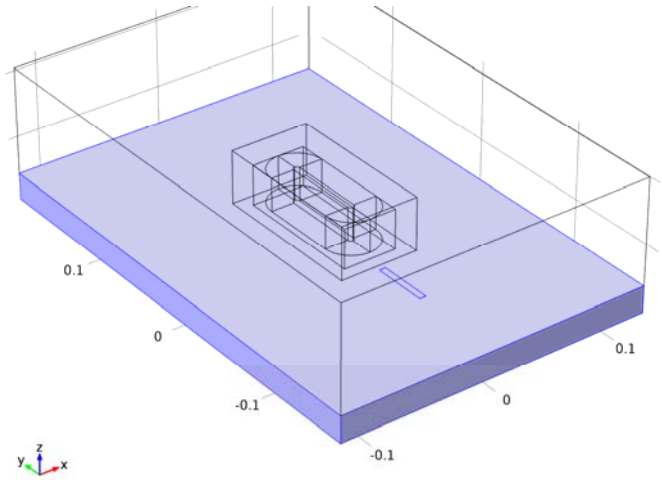

Pic. 15. Model of whole system in COMSOL Multiphysics (dimensions given in meters)

Pic. 16 shows the time evolution of temperatures along the line UV indicated in Pic. 7 at several different times. The horizontal axis is connected with the system inductor-laser.

The blue line shows the temperature profile after 30 s from the beginning of movement (the state is still unsteady). The green line shows the state after 60 s of heating (the system moved by 60 mm from the initial position) and the red line shows the profile after 120 s, when the process can be considered in a steady state. It can be seen that in the

steady state, the pre-heating temperature reaches about 350 °C, then it somewhat decreases behind the inductor and finally it rises to about 1350 °C after heating by the laser beam. The steady-state profile is already quite acceptable.

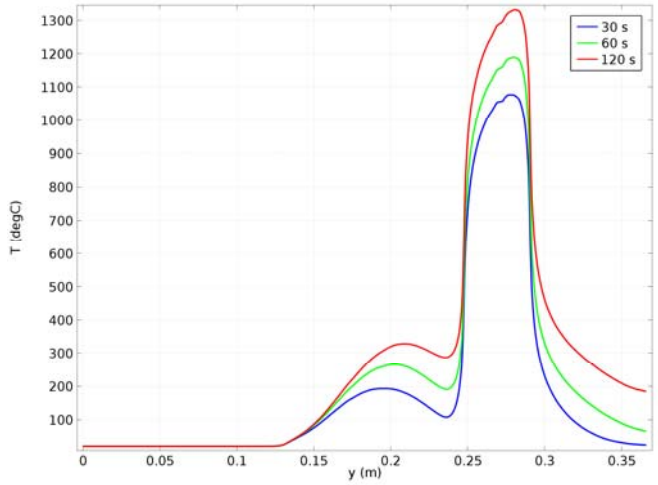

Pic. 16. Time evolution of temperatures along the line UV on the surface in three different times

Pics. 17 and 18 show analogous temperature profiles not only along the surface, but also in specified depths (1 mm, 2 mm and 3 mm) in it at the given time instants.

Pic. 17 shows this profile after 30 s of heating. It is clear that only a very thin surface layer of the plate is able to be hardened at this time, because the temperatures in depths exceeding 1 mm do not reach the austenitizing temperature Ac_3. Analogous is the state after 60 s of heating shown in Pic. 18. The situation is better only in the steady state after about 120 s of heating, where the maximum temperature reaches 1100 °C, which is already sufficient for hardening.

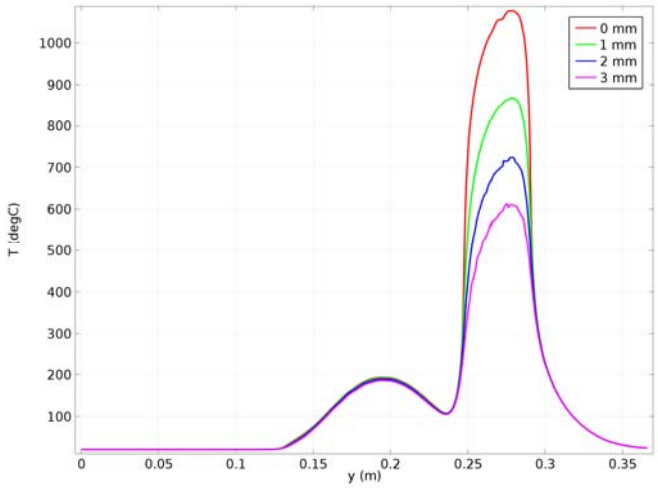

Pic. 17. Time evolution of temperatures along the line UV in several depths of the plate after 30 s of heating

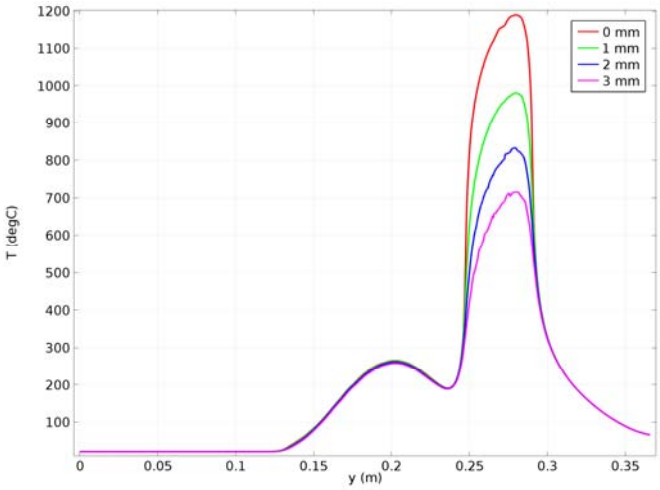

Pic. 18. Time evolution of temperatures along the line UV in several depths of the plate after 60 s of heating

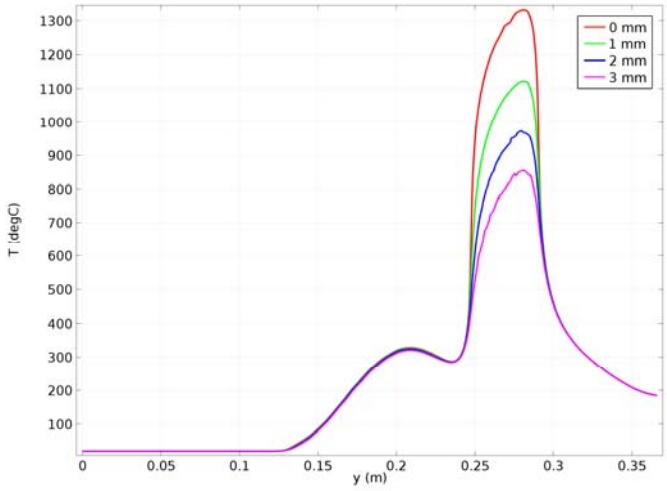

Pic. 19. Time evolution of temperatures along the line UV in several depths of the plate after 120 s of heating

Finally, Pic. 20 shows the distribution of the steady-state surface temperature after 120 s of heating.

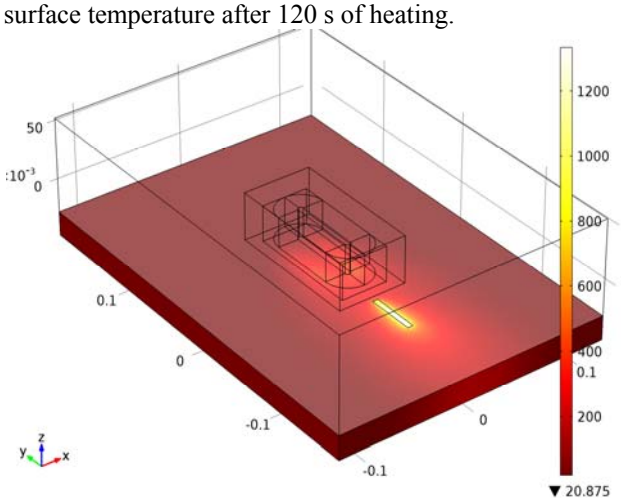

Pic. 20. Steady-state distribution of surface temperature

CONCLUSION

The paper presents a mathematical model of a combined heating process by the classic inductor and laser beam and

several interesting results of a typical illustrative example. It is clear that this way of heating results in quite an acceptable temperature profile of the heated path that is appropriate for reducing undesirable mechanical stresses in the surface layers of material due to excessive temperature gradients.

Further work will be aimed at the improvement of the time evolution of cooling. Although fast cooling is desirable from the viewpoint of higher hardness, its velocity should be somewhat smaller. It can be reached by an appropriate post-heating of the body using another inductor (or both pre-heating and post-heating may be performed by only one specially formed inductor).

ACKNOWLEDGMENT

Financial support of the project TACR TA03010354 is highly acknowledged.

BIBLIOGRAPHY

1. Ashby, M. F., Easterling, K. A. The Transformation Hardening of Steel Surfaces by Laser Beams – I. Hypo-Eutectoid Steels – Acta Metallurgica 32 (1984), No. 11, pp. 1935–1948.
2. Yánez, A, Álvarez, J. C., López, A. J., Nicolás, G., Pérez J. A., Ramil, A., Saavedra, E. Modelling of Temperature Evolution on Metals During Laser Hardening Process – Applied Surface Science 186 (2002), No. 1–4, pp. 611–616.
3. Kuczmann, M., Ivanyi, A. The Finite Element Method in Magnetics. Akademiai Kiado, Budapest, 2008.
4. Stratton, J. A. Electromagnetic Theory, Wiley-IEEE Press, 2007.
5. Bird, J. Modeling a 3D Eddy Current Problem Using the Weak Formulation of the Convective $\boldsymbol{A}$ - φ Steady State Method. Proc. COMSOL Conference, Boston, 2009.
6. Li, Y., Berthiau, G., Feliachi, M., Cheriet, A. 3D Finite Volume Modeling of ENDE Using Electromagnetic $\boldsymbol{T}$-Formulation. Journal of Sensors, 2012, article ID 785271.
7. Holman, J. P. Heat Transfer, McGraw-Hill, New York, 2002.
8. URL: www.comsol.com.